Nova Publishers

Smart Grid: Technologies, Applications and Management Systems

Accurate Component Model Based Control Algorithm for Residential Photovoltaic and Energy Storage Systems Accounting for Prediction Inaccuracies

Yanzhi Wang, Xue Lin, Massoud Pedram

Dept. of EE, University of Southern California, Los Angeles, CA 90089, USA

Corresponding author email: yanzhiwa@usc.edu

Abstract

Integrating residential photovoltaic (PV) power generation and energy storage systems into the Smart Grid is an effective way of utilizing renewable power and reducing the consumption of fossil fuels. This has become a particularly interesting problem with the introduction of dynamic electricity energy pricing models, since electricity consumers can utilize their PV-based energy generation and controllable energy storage devices for peak shaving on their power demand profile from the Smart Grid, and thereby, minimize their electricity bill cost. A realistic electricity pricing function is considered in this chapter with the billing period of a month, which is comprised of both an energy price component and a demand price component. Due to the characteristics of the realistic electricity price function and the energy storage capacity limitation, the residential storage control algorithm should (i) effectively take into account the PV power generation and load power consumption prediction results and mitigate the inevitable inaccuracy in these predictions, and (ii) properly account for various energy loss components during system operation, including the energy loss components due to rate capacity effect in the storage system as well as power dissipation in the power conversion circuitries. A near-optimal storage control algorithm is proposed accounting for these aspects, based on the PV power generation and load power consumption prediction methods in the previous papers. The near-optimal control algorithm, which controls the charging/discharging schemes of the storage system, is effectively implemented by solving a convex optimization problem at the beginning of each day with polynomial time complexity. The optimal size of the energy storage system is determined in order to minimize the break-even time of the initial investment in the

PV and storage systems. Experimental results demonstrate the effectiveness of the proposed near-optimal residential storage control algorithm in electricity cost reduction compared with the baseline control algorithm.

Keywords: Residential user; photovoltaic system; energy storage; adaptive control; component model; prediction error.

---

1. Introduction

The traditional (static and centrally controlled) structure of power grid is comprised of a transmission network, which transmits electricity power generated at remote power plants to substations through long-distance and high-voltage transmission lines, and a distribution network, which delivers electrical power from substations to local end users/consumers. In this infrastructure, the local distribution network is often statically adjusted to match the load profile of its end users. Since the end user profiles often change phenomenally according to the day of week and time of day, the Power Grid must be able to support the worst-case power demands of all the end users at all times in order to avoid potential power delivery failure (blackout or brownout) [2].

The decentralized *Smart Grid* infrastructure is being designed to avoid expending a large amount of capital for increasing the power generation capacity of utility companies in order to meet the expected growth of end user energy consumptions in the worst case [3], [4]. The Smart Grid is also being equipped with smart meters, which can monitor and control the power flow in the power grid to match the amount of power generation to that of power consumption, and to minimize the overall cost of electrical energy delivered to end users.

In the Smart Grid infrastructure, utility companies can employ *dynamic electricity pricing* strategies, that is, they employ different electricity prices at different time periods in a day or at different locations. This policy will incentivize energy consumers to perform *demand side management*, also known as *demand response*, by adjusting their power demand from the Grid to match the power generation capacity of the Grid. There are several ways to perform such a demand side management, including the integration of intermittent energy sources such as photovoltaic (PV) power or wind power at the residential level, demand shaping (i.e., consumers shift their tasks to the off-peak periods), household task scheduling, etc. [5]. In this paper, we focus on the

former solution, or more specifically, integrating PV power generation facilities with the Smart Grid for residential usage.

Although integrating residential renewable energy sources into the Smart Grid proves to be an effective way of utilizing renewable power and reducing the usage of fossil fuels, several problems need to be addressed for these benefits to be realized. First, there exists a mismatch between the peak PV power generation time (usually around noon) and the peak load power consumption time for residential users (usually in the evening) in each day [6]. This timing skew results in cases where the generated PV power cannot be optimally utilized for peak power shaving. Moreover, at each time instance, the PV output power is fixed depending on the solar irradiance level, when employing the MPPT or MPTT control methods [8], [9]. Hence, the ability of the residential user for peak load shaving is also restricted by the PV output power.

One effective solution to the above-mentioned problems is to incorporate energy storage systems, either homogeneous or hybrid, for houses equipped with PV systems [1], [6]. The proposed residential energy storage system shall store power from the Smart Grid during off-peak periods of each day and (or) from the PV system, and provide power for the end users during the peak periods of that day for peak power shaving and energy cost reduction (since electrical energy tends to be the most expensive during these peak hours.) Therefore, the design of energy pricing-aware control algorithms for the residential storage system, which controls the charging and discharging of the energy storage bank(s) and the magnitude of the charging/discharging current, is an important task in order for the Smart Grid technology to deliver on its promises.

Effective storage control algorithms should take into account the realistic electricity pricing function, such as [10], [11]. It is comprised of both an *energy price* component which is a time of usage (TOU) dependent function indicating the unit energy price during each time periods of the billing period (a day, or a month, etc.), and a *demand price* component, which is an additional charge due to the peak power consumption in the billing period. The latter component is required in order to prevent a case whereby all the customers utilize their PV power generation and energy storage systems and/or schedule their loads such that a very large amount of power is demanded from the Smart Grid during low-cost (off peak) time slots, which can subsequently result in power delivery failures.

The capacity/size of the storage system is limited due to the relatively high cost of electrical energy storage elements. Therefore, the following three requirements need to be satisfied so that the storage controller can perform optimization of the total cost induced by both the energy price and the demand price. First, at each decision epoch of a billing period, it is important for the controller to forecast the PV power generation and load power consumption profiles. Second, the storage control algorithm should effectively mitigate the inevitable prediction error in PV and load power predictions. Third, the storage control algorithm should accurately account for the energy loss in the storage charging/discharging process and in power conversion circuitry to achieve optimality in the total cost saving. This requirement implies taking into account accurate energy loss in the storage charging/discharging process and in power conversion circuitry to achieve optimality in total cost saving. This requirement implies taking into account accurate energy loss models for storage and power conversion circuitry in the controller's optimization framework. To satisfy the first requirement, references [12], [13], and [14] are representatives of general PV power generation and load power consumption predictions by either forecasting the complete power profiles, or certain statistical characteristics of the power profiles. Prediction techniques include (but are not limited to): machine learning-based, ant colony clustering-based, and residential activity-based methods. In [6], we have presented PV and load power profiles prediction algorithms specifically designed for the Smart Grid residence. On the other hand, few research papers have focused on addressing the second and third requirements.

In this paper, we consider the case of a Smart Grid residential user equipped with local PV power generation and an energy storage system. We consider a realistic electricity price function comprised of both energy and demand prices, with system architecture and the storage power loss model used in the paper. Based on the PV power generation and load power consumption prediction results from previous papers, we present a near-optimal storage control algorithm that mitigates the inevitable prediction errors and properly accounts for the energy loss components due to power dissipation in the power conversion circuitries, as well as the rate capacity effect, which is the most significant portion of energy loss in the storage system. The proposed near-optimal storage control algorithm is effectively implemented by solving a convex optimization problem with polynomial time complexity at the beginning of each day in a billing period. Experimental results demonstrate that the

proposed residential storage control algorithm achieves up to 2.62X enhancement in electricity cost reduction compared with the baseline storage control algorithm.

The remainder of this chapter is organized as follows. We describe the system modeling, price function, and overall cost function in Section 2. Section 3 presents the power loss modeling of the storage system. Section 4 presents the residential storage control algorithm to compensate prediction error and minimize the total energy cost over a billing period. Experimental results and conclusion are presented in Section 5 and Section 6, respectively.

2. System Modeling and Cost Function

In this paper, we consider an individual Smart Grid residential user that is equipped with PV power generation and energy storage systems, as shown in Fig. 1. The PV system and storage system are connected to a *residential DC bus*, via unidirectional and bidirectional DC-DC converters, respectively. An AC bus, which is further connected to the Smart Grid, is connected via an AC/DC interface (e.g., inverter, rectifier, and transformer circuitry) to the residential DC bus. The residential AC load (e.g. household appliances, lighting and heating equipments) is connected to the AC bus. In this chapter, we consider the power losses in the above-mentioned power conversion circuitry for the realistic concern.

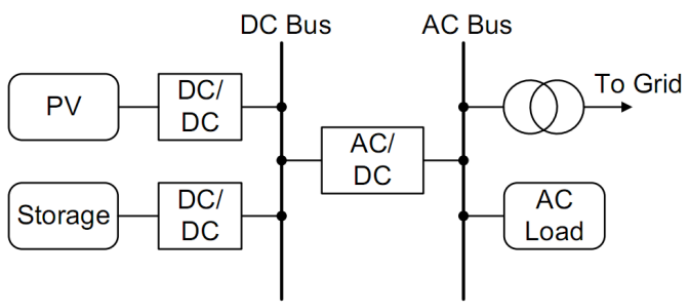

Fig. 1. Block diagram illustrating the interface between the PV module, storage system, residential load, and the Smart Grid.

We adopt a *slotted time* modeling approach, i.e., all system constraints as well as decisions are provided for discrete time intervals of equal and constant length. More specifically, each day is divided into T time slots, each with a duration of D. We use $T = 96$ and $D = 15$ minutes. Let set $\boldsymbol{S}$ denote the set of all T time slots in each day.

We adopt a realistic electricity price function comprised of both the energy price component and the demand price component as discussed before, with a billing period of a month [10]. Consider a specific day *i* of a billing period. The residential load power consumption at the j^{th} time slot of that day is denoted by $P_{load,i}[j]$. The output power levels of PV and storage systems at the j^{th} time slot are denoted by $P_{pv,i}[j]$ and $P_{st,i}[j]$, respectively. Notice that, $P_{st,i}[j]$ may be positive (discharging from the storage), negative (charging the storage), or zero.

We assume that the PV power generation $P_{pv,i}[j]$ can be accurately predicted at the beginning of the i^{th} day based on the PV power generation characteristics. On the other hand, the residential load power consumption $P_{load,i}[j]$ cannot be accurately predicted, and let $\hat{P}_{load,i}[j]$ denote the predicted value of $P_{load,i}[j]$ in the j^{th} time slot in the i^{th} day. We use $P_{grid,i}[j]$ to denote the power required from the Smart Grid, i.e., the *grid power*, at the j^{th} time slot of the i^{th} day, where $P_{grid,i}[j]$ can be positive (if the Smart Grid provides power for the residential usage), negative (if the residential system sells power back into the Smart Grid), or zero. Similarly, we use $\hat{P}_{grid,i}[j]$ to denote the predicted value of $P_{grid,i}[j]$.

We consider realistic power conversion circuitry (i.e., their power conversion efficiency is less than 100%) in the proposed optimization framework. Accordingly, we use η_1, η_2, and η_3 to denote the power conversion efficiencies of the DC-DC converter between the PV system and the DC bus, the DC-DC converter connecting between the storage system and the DC bus, and the AC/DC power conversion interface, respectively. Those power conversion efficiency values are typically in the range of 85% to 95%.

There are three *operating modes* in the system. In the first mode, both the PV system and the storage system are providing power for the residential load (i.e., the storage system is being discharged.) For the j^{th} time slot of the i^{th} day, the condition that the residential system is in the first mode is given by $P_{st,i}[j] \geq 0$. In this mode, the actual grid power $P_{grid,i}[j]$ can be calculated by:

$$P_{grid,i}[j] = P_{load,i}[j] - \eta_1 \cdot \eta_3 \cdot P_{pv,i}[j] - \eta_2 \cdot \eta_3 \cdot P_{st,i}[j] \quad (1)$$

whereas the predicted grid power $\hat{P}_{grid,i}[j]$ is given by:

$$\hat{P}_{grid,i}[j] = \hat{P}_{load,i}[j] - \eta_1 \cdot \eta_3 \cdot P_{pv,i}[j] - \eta_2 \cdot \eta_3 \cdot P_{st,i}[j] \quad (2)$$

In the second mode, the storage system is being charged, and the PV system is sufficient for charging the storage. For the j^{th} time slot of the i^{th} day, the condition that the residential system is in the second mode is given by $P_{st,i}[j] < 0$ and $\eta_1 P_{pv,i}[j] + \frac{1}{\eta_2} P_{st,i}[j] \geq 0$. In this mode, there is power flowing from the DC bus to the AC bus, and the actual grid power can be calculated by:

$$P_{grid,i}[j] = P_{load,i}[j] - \eta_1 \eta_3 \cdot P_{pv,i}[j] - \frac{\eta_3}{\eta_2} \cdot P_{st,i}[j] \tag{3}$$

whereas the predicted grid power $\hat{P}_{grid,i}[j]$ is given by:

$$\hat{P}_{grid,i}[j] = \hat{P}_{load,i}[j] - \eta_1 \eta_3 \cdot P_{pv,i}[j] - \frac{\eta_3}{\eta_2} \cdot P_{st,i}[j] \tag{4}$$

In the third mode, the storage system is being charged, and the PV system is insufficient for charging the storage. In other words, the storage is simultaneously charged by the PV system and the Grid. For the j^{th} time slot of the i^{th} day, the condition that the residential system is in the third mode is given by $P_{st,i}[j] < 0$ and $\eta_1 P_{pv,i}[j] + \frac{1}{\eta_2} P_{st,i}[j] < 0$. In this mode, there is power flowing from the AC bus to the DC bus, and the actual grid power is given by:

$$P_{grid,i}[j] = P_{load,i}[j] - \frac{1}{\eta_3} \cdot \left(\eta_1 P_{pv,i}[j] + \frac{1}{\eta_2} P_{st,i}[j] \right) \tag{5}$$

whereas the predicted grid power $\hat{P}_{grid,i}[j]$ is given by:

$$\hat{P}_{grid,i}[j] = \hat{P}_{load,i}[j] - \frac{1}{\eta_3} \cdot \left(\eta_1 P_{pv,i}[j] + \frac{1}{\eta_2} P_{st,i}[j] \right) \tag{6}$$

It can be observed from the above equations (1) - (6) that $P_{grid,i}[j]$ (or $\hat{P}_{grid,i}[j]$) is a piecewise linear (continuous) and monotonically decreasing function of $P_{st,i}[j]$, when $P_{pv,i}[j]$ and $P_{load,i}[j]$ (or $\hat{P}_{load,i}[j]$) values are given. $P_{grid,i}[j]$ (or $\hat{P}_{grid,i}[j]$) is also a convex function of $P_{st,i}[j]$.

As specified in [10] and [11], the electricity price function is pre-announced by the utility company just before the start of each billing period, and it will not change until possibly the start of the next billing period. We use a general electricity price function as follows. We use $Price_E[j]$ to denote the unit energy price at the j^{th} time slot of a day. Then the cost we actually pay in a billing period due to the energy price component is given by:

$$Cost_E = \sum_{i=1}^{30} \sum_{j=1}^{96} Price_E[j] \cdot P_{grid,i}[j] \cdot D \quad (7)$$

The demand price component, on the other hand, is charged for the peak power drawn from the Grid over certain time periods in a billing period. A generic definition of the demand price is given as follows. Let $\boldsymbol{S}_1$, $\boldsymbol{S}_2$, ..., $\boldsymbol{S}_N$ be N different non-empty subsets of the original set $\boldsymbol{S}$ of time slots, each of which corresponds to a specific time period, named by the term *price periods*, in a day. A price period does not necessarily need to be continuous in time. For example, a price period can span from 10:00 to 12:59 and then from 17:00 to 19:59, as shown in [10]. Also those price periods in a day do not need to be mutually exclusive. We use $j \in \boldsymbol{S}_k$ to denote the statement that the j^{th} time slot in a day belongs to the k^{th} price period. Let $Price_{D,k}$ denote the demand price charged over each k^{th} price period $\boldsymbol{S}_k$. Then the cost we have to pay in a billing period due to the demand price component is given by

$$Cost_D = \sum_{k=1}^{N} Price_{D,k} \cdot \max_{1 \le i \le 30, j \in \boldsymbol{S}_k} P_{grid,i}[j] \quad (8)$$

Obviously, the actual total cost for the residential user in a billing period (i.e., a month) is the summation of the two aforesaid cost components.

3. The Storage Power Modeling

The most significant cause of power losses in the storage system, which is typically made of lead-acid batteries or Li-ion batteries, is the rate capacity effect of batteries [15]. To be more specific, high discharging current of the battery will reduce the amount of available energy that can be extracted from the battery, thereby reducing the battery's service life between fully charged and fully discharged states [15]. In other words, high-peak pulsed discharging current will deplete much more of the battery's stored energy than a smooth workload with the same total energy demand. We use *discharging efficiency* of a battery to denote the ratio of the battery's output current to the degradation rate of its stored charge. Then the rate capacity effect specifies the fact that the discharging efficiency of a battery decreases with the increase of the battery's discharging current. The rate capacity effect also affects the energy loss in the battery during the charging process in a similar way.

The rate capacity effect can be captured using the Peukert's formula, an empirical formula specifying the battery charging and discharging efficiencies as functions of the charging current I_c and discharging current I_d, respectively:

$$\eta_{rate,c}(I_c) = \frac{1}{(I_c/I_{ref})^{\alpha_c}}, \quad \eta_{rate,d}(I_d) = \frac{1}{(I_d/I_{ref})^{\alpha_d}} \tag{9}$$

where α_c and α_d are peukert's coefficients, and their values are typically in the range of 0.1 - 0.3; I_{ref} denotes the *reference current* of the battery, which is proportional to the battery's nominal capacity C_{nom}. Typically, I_{ref} is set to $C_{nom}/20$, indicating that it takes 20 hours to fully discharge the battery using discharging current I_{ref}.

We name I_c/I_{ref} and I_d/I_{ref} the battery's *normalized charging current* and *normalized discharging current*, respectively. Notice that the efficiency values $\eta_{rate,c}(I_c)$ and $\eta_{rate,d}(I_d)$ in Eqn. (9) are greater than 100% if the magnitude of the normalized charging or discharging current is less than one, which implies that the above-mentioned Peukert's formula is not accurate in this case. We modify the Peukert's formula such that the efficiency values $\eta_{rate,c}(I_c)$ and $\eta_{rate,d}(I_d)$ become equal to 100% if the magnitude of the normalized charging/discharging current is less than one. In other words, the battery suffers from no rate capacity effect in this case.

We denote the increase/degradation rate of storage energy in the j^{th} time slot of the i^{th} day by $P_{st,in,i}[j]$, which may be positive (i.e., discharging from the storage, and the amount of stored energy decreases), negative (i.e., charging the storage, and the amount of stored energy increases), or zero. Based on the modified Peukert's formula, the relationship between $P_{st,in,i}[j]$ and the storage output power $P_{st,i}[j]$ is given by:

$$P_{st,i}[j] = \begin{cases} V_{st} \cdot I_{st,ref} \cdot \left(\frac{P_{st,in,i}[j]}{V_{st} \cdot I_{st,ref}}\right)^{\beta_1}, \text{if } \frac{P_{st,in,i}[j]}{V_{st} \cdot I_{st,ref}} > 1 \\ P_{st,in,i}[j], \text{ if } -1 \le \frac{P_{st,in,i}[j]}{V_{st} \cdot I_{st,ref}} \le 1 \\ -V_{st} \cdot I_{st,ref} \cdot \left(\frac{|P_{st,in,i}[j]|}{V_{st} \cdot I_{st,ref}}\right)^{\beta_2}, \text{if } \frac{P_{st,in,i}[j]}{V_{st} \cdot I_{st,ref}} < -1 \end{cases} \tag{10}$$

where V_{st} is the storage terminal voltage and is supposed to be (near-) constant; $I_{st,ref}$ is the reference current of the storage system, which is proportional to its nominal capacity $C_{st,nom}$ given in Ampere-Hour (Ahr); coefficient β_1 is in the range of 0.8 - 0.9, whereas coefficient β_2 is in the range of 1.1 - 1.3.

One can observe that when the storage discharging (or charging) current is the same, the discharging (or charging) efficiency becomes higher (i.e., the rate capacity effect becomes less significant) when the nominal capacity of the storage system is larger.

We use the function $P_{st,i}[j] = f_{st}\left(P_{st,in,i}[j]\right)$ to denote the relationship between $P_{st,i}[j]$ and $P_{st,in,i}[j]$. An important observation is that such a function is a concave and monotonically increasing function over the input domain $-\infty < P_{st,in,i}[j] < \infty$, as shown in Fig. 2. Due to the monotonicity property, $P_{st,in,i}[j]$ is also a monotonically increasing function of $P_{st,i}[j]$, denoted by $P_{st,in,i}[j] = f_{st}^{-1}\left(P_{st,i}[j]\right)$. We can see from Fig. 2 that a lead-acid battery-based storage system has more significant energy loss due to rate capacity effect than a Li-ion battery-based storage system. However, the lead-acid battery-based storage system is more often deployed in real household scenarios due to cost considerations (the capital cost of lead-acid battery is only 100 - 200 $/kWh, whereas that of Li-ion battery is > 600 $/kWh [16].)

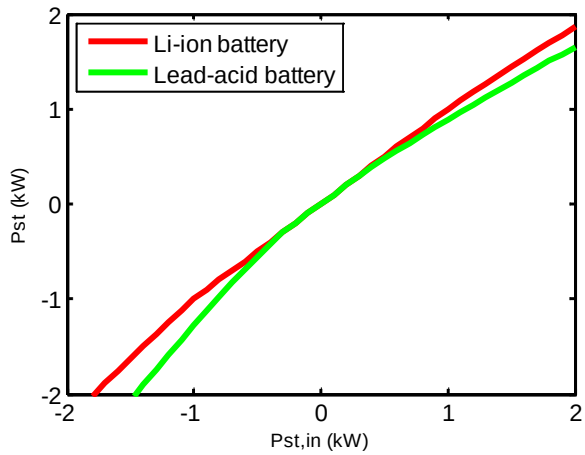

Fig. 2. Relationship between $P_{st,i}[j]$ and $P_{st,in,i}[j]$ in two types in two types of batteries.

4. Optimal Control Algorithm of Residential Storage System

In this section, we introduce in details the proposed near-optimal residential storage control algorithm accounting for prediction inaccuracy, which could effectively utilize the combination of PV power generation and load power consumption prediction results to minimize the total electricity cost, including both the energy price and the demand price, over each billing period (i.e., a month.)

The storage control optimization problem is performed at time 00:00 (i.e., at the beginning) of each day in the billing period. To be more realistic, we assume that the prediction results of PV power generation and load power consumption profiles of each i^{th} day are not available before time 00:00 of that day. We further assume that the PV power generation profile at each day, i.e., $P_{pv,i}[j]$ for $1 \leq j \leq 96$, can be accurately predicted from

the weather forecast and prediction algorithms presented in our previous work [6]. On the other hand, the load power consumption profile $\hat{P}_{load,i}[j]$ for $1 \le j \le 96$ is not perfectly accurate. We assume that $\hat{P}_{load,i}[j]$ follows a uniform distribution over the range of $\left[P_{load,i}[j] - \delta, P_{load,i}[j] + \delta\right]$, in which the average value $P_{load,i}[j]$ is the actual load power consumption and δ can be estimated from the previous (observed) load power consumption profiles. Hence, with given predicted value $\hat{P}_{load,i}[j]$, $P_{load,i}[j]$ also follows a uniform distribution over the range of $\left[\hat{P}_{load,i}[j] - \delta, \hat{P}_{load,i}[j] + \delta\right]$. At time 00:00 of each i^{th} day, the storage controller performs optimization to find the optimal storage system output power profile $P_{st,i}[j]$ for $1 \le j \le 96$ throughout the day, which is equivalent to finding the charging/discharging current profile of the storage system.

In this section, we first introduce the storage control optimization performed at the beginning of a billing period (i.e., at time 00:00 of day $i = 1$), in order to achieve a balance between the expected $Cost_E$ (induced by the energy price component) and expected $Cost_D$ (induced by the demand price component) values. In this way, we can minimize the total expected energy cost. Next, we introduce the storage control optimization performed at the beginning of the other days in the billing period, properly taking into account the prediction errors.

Although in reality we control the output power $P_{st,i}[j]$ $(1 \le i \le 30,\ 1 \le j \le 96)$ of the storage system during the system operation, we use $P_{st,in,i}[j]$ $(1 \le i \le 30,\ 1 \le j \le 96)$ as the control variables in the optimal storage control problem formulation because it can help transform the optimal storage control problem into a standard convex optimization problem. We observe from Eqns. (1), (3), (5), and (10) that the grid power $P_{grid,i}[j]$ $(1 \le i \le 30,\ 1 \le j \le 96)$ is a monotonically decreasing function of $P_{st,in,i}[j]$, denoted by $P_{grid,i}[j] = f_{grid}\left(P_{st,in,i}[j]\right)$, over the input domain $-\infty < P_{st,in,i}[j] < \infty$. Furthermore, $P_{grid,i}[j] = f_{grid}\left(P_{st,in,i}[j]\right)$ is a convex function of the control variable $P_{st,in,i}[j]$ according to the rules of convexity in function compositions [18], because of the following two reasons: (i) $P_{grid,i}[j]$ is a convex and monotonically decreasing function of $P_{st,i}[j]$, and (ii) $P_{st,i}[j] = f_{st}\left(P_{st,in,i}[j]\right)$ is a concave function of $P_{st,in,i}[j]$. Similarly, the estimated grid power $\hat{P}_{grid,i}[j]$ $(1 \le i \le 30,\ 1 \le j \le 96)$ is also a monotonically decreasing function of $P_{st,in,i}[j]$, denoted by $\hat{P}_{grid,i}[j] = \hat{f}_{grid}\left(P_{st,in,i}[j]\right)$.

At any time in a billing period, let $Peak_k$ $(1 \le k \le N)$ denote the peak grid power consumption value that is *observed so far* over the k^{th} price period in the billing period of interest (cf. Section 2). Obviously, such $Peak_k$

values are initialized to zero at the beginning of the billing period, and are updated at the end of each day according to the actual (observed) grid power consumption profiles.

4.1. Storage Control Optimization at the Beginning of a Billing Period

In this section, we introduce the storage control optimization performed at the beginning of a billing period (i.e., at time 00:00 of day $i = 1$), in order to achieve a desirable balance between the expected $Cost_E$ and expected $Cost_D$ values. At that time, we have $Peak_k = 0$ for $1 \le k \le N$. The storage controller is only aware of the PV power generation and load power consumption predictions in the 1st day of the billing period, i.e., $P_{pv,1}[j]$ and $\hat{P}_{load,1}[j]$ for $1 \le j \le 96$, in which $\hat{P}_{load,1}[j]$ is inaccurate. The storage control derives the optimal $P_{st,in,1}[j]$ profile for $1 \le j \le 96$. The objective of the storage controller is to minimize an estimation of the total electricity cost in the billing period. Then the Optimal Storage Control problem performed at the Beginning of a billing period (the OSC-B problem) is formally described as follows:

The OSC-B Problem Formulation

Given the PV power generation profiles of the 1st day in the billing period, i.e., $P_{pv,1}[j]$ for $1 \le j \le 96$, the predicted load power consumption profiles $\hat{P}_{load,1}[j]$ for $1 \le j \le 96$, and the initial energy $E_{st,ini,1}$ in the storage system at time 00:00.

Find the optimal $P_{st,in,1}[j]$ profile for $1 \le j \le 96$.

Minimize an estimation of the total electricity cost in the billing period, which is given by:

$$Cost_D + Cost_E = 30 \cdot \sum_{j=1}^{96} Price_E[j] \cdot \hat{P}_{grid,1}[j] \cdot D + \sum_{k=1}^{N} Price_{D,k} \cdot \max\left(Peak_k, \max_{j \in \boldsymbol{S}_k} \hat{P}_{grid,1}[j] + \delta\right) \quad (11)$$

Subject to the following constraints:

For each $1 \le j \le 96$:

$$-P_{MAX,c} \le P_{st,in,1}[j] \le P_{MAX,d} \quad (12)$$

$$0 \le E_{st,ini,1} - \sum_{l=1}^{j} P_{st,in,1}[l] \cdot D \le E_{st,full} \quad (13)$$

$$E_{st,ini,1} - \sum_{j=1}^{96} P_{st,in,1}[j] \cdot D \ge E_{st,ini,1} \quad (14)$$

In the OSC-B problem formulation, the objective function (11) is an estimation of the total electricity cost in the whole billing period. In this equation, we use the predicted PV power generation and load power consumption profiles of the first day, i.e., $P_{pv,1}[j]$ and $\hat{P}_{load,1}[j]$ for $1 \leq j \leq 96$, as a representation for the whole billing period. This is because the storage controller can only predict the PV power generation and load power consumption profiles in the first day. Moreover, in the objective function (11), we use $\hat{P}_{grid,1}[j] + \delta$ as an estimation of the expected value of $\max_i P_{grid,i}[j]$. This is because of the assumption that $P_{grid,i}[j]$ is uniformly distributed over the range of $\left[\hat{P}_{grid,i}[j] - \delta, \hat{P}_{grid,i}[j] + \delta\right]$ in the OSC-B problem formulation.

In the OSC-B problem, constraint (12) represents the restrictions on the maximum allowable amount of power flowing into and out of the storage system during charging and discharging, respectively. Constraint (13) ensures that the storage energy can never become less than zero or exceed a maximum value $E_{st,full}$ throughout the day. Finally, constraint (14) ensures that the remaining storage energy at the end of day, which is required for performing peak power shaving on the next day, is no less than the initial value $E_{st,ini,1}$.

The OSC-B problem is a standard convex optimization problem due to the following two reasons:

- The objective function (11) is a convex objective function because the pointwise maximum function of a set of convex functions is still a convex function.
- The other constraints are all convex (or linear) inequality constraints of optimization variables.

Although the OSC-B problem is formulated as a convex optimization problem, and therefore, it can be solved optimally with a polynomial time complexity using convex optimization algorithms [18], [19], it is difficult to directly solve the OSC-B problem by using standard convex optimization tools such as CVX [19] or the *fmincon* function in MATLAB. This is because the function $\hat{P}_{grid,i}[j] = \hat{f}_{grid}\left(P_{st,in,i}[j]\right)$ is non-differentiable at several points, and typical convex optimization tools only accept differentiable objective functions. To address this issue, we use a piecewise linear function to approximate the function $\hat{f}_{grid}\left(P_{st,in,i}[j]\right)$, and then transform the OSC-B problem into a linear programming problem (please note that all the constraints are linear constraints), which could be optimally solved using standard optimization tools in polynomial time complexity. Details are omitted due to space limitation. Similar method will also be applied to the optimal storage control problem as shall be discussed in Section 4.2.

4.2. Storage Control Optimization at the Beginning of the Other Days

We introduce the storage control optimization at the beginning of the other days in the billing period (i.e., days 2, 3, and so on). Suppose that we are at the beginning of the i^{th} day of the billing period of interest. At that time, the $Peak_k$ values may not be zero any more. The storage controller is aware of the accurate PV power predictions and inaccurate load power consumption predictions in the i^{th} day, i.e., $P_{pv,i}[j]$ and $\hat{P}_{load,i}[j]$ for $1 \le j \le 96$. The storage controller derives the optimal $P_{st,in,i}[j]$ profile for $1 \le j \le 96$. The objective of the storage controller is to minimize the *expected increase of the electricity cost* in the i^{th} day of the billing period, as will be formally described as follows. The Optimal Storage Control problem performed at the beginning of the Other days in the billing period (the OSC-O problem) is formally described as follows:

The OSC-O Problem Formulation

Given the PV power generation profiles of the i^{th} day in the billing period, i.e., $P_{pv,i}[j]$ for $1 \le j \le 96$, the predicted load power consumption profiles $\hat{P}_{load,i}[j]$ for $1 \le j \le 96$, and the initial energy $E_{st,ini,i}$ in the storage system at time 00:00.

Find the optimal $P_{st,in,i}[j]$ profile for $1 \le j \le 96$.

Minimize the estimated increase in the electricity cost in the i^{th} day, which is given by

$$\sum_{j=1}^{96} Price_E[j] \cdot \hat{P}_{grid,i}[j] \cdot D + \sum_{k=1}^{N} Price_{D,k} \cdot \left(\max\left(Peak_k, \max_{j \in \boldsymbol{S}_k} \frac{Peak_k + \hat{P}_{grid,i}[j] + \delta}{2} \right) - Peak_k \right) \quad (15)$$

or equivalently, minimize

$$\sum_{j=1}^{96} Price_E[j] \cdot \hat{P}_{grid,i}[j] \cdot D + \sum_{k=1}^{N} Price_{D,k} \cdot \max\left(Peak_k, \max_{j \in \boldsymbol{S}_k} \frac{Peak_k + \hat{P}_{grid,i}[j] + \delta}{2} \right) \quad (16)$$

Subject to the following constraints:

For each $1 \le j \le 96$:

$$-P_{MAX,c} \le P_{st,in,i}[j] \le P_{MAX,d} \quad (17)$$

$$0 \le E_{st,ini,i} - \sum_{l=1}^{j} P_{st,in,i}[l] \cdot D \le E_{st,full} \quad (18)$$

$$E_{st,ini,i} - \sum_{j=1}^{96} P_{st,in,i}[j] \cdot D \ge E_{st,ini,i} \quad (19)$$

In the OSC-O problem formulation, the objective function (15) is an estimation of the increase of the electricity cost in the i^{th} day of the billing period of interest. The objective function is comprised of two parts: (i)

the expected energy price-induced electricity cost in the i^{th} day of the billing period, given by the first term $\sum_{j=1}^{96} Price_E[j] \cdot \hat{P}_{grid,i}[j] \cdot D$ of Eqn. (15), and (ii) the estimation of the increase in demand price-induced electricity cost in the billing period of interest, given by the second term $\sum_{k=1}^{N} Price_{D,k} \cdot \left(\max\left(Peak_k, \max_{j \in \boldsymbol{S}_k} \frac{Peak_k + \hat{P}_{grid,i}[j]+\delta}{2}\right) - Peak_k\right)$ of Eqn. (15). In the second term, we use $\frac{Peak_k + \hat{P}_{grid,i}[j]+\delta}{2}$ as a (conservative) estimation of the expected value of $\max(Peak_k, P_{grid,i}[j])$ when $\hat{P}_{grid,i}[j] + \delta \geq Peak_k$. Please note that $P_{grid,i}[j]$ is uniformly distributed over the range of $\left[\hat{P}_{grid,i}[j] - \delta, \hat{P}_{grid,i}[j] + \delta\right]$ in the problem formulation. Moreover, the constraints in the OSC-O problem are similar to the constraints in the OSC-B problem as discussed in Section 4.1.

Again, similar to the above-mentioned OSC-B problem, the OSC-O problem has a convex objective function (15) or (16), and linear inequality constraints (17) - (19), of the optimization variables. Therefore, the OSC-O problem can also be optimally solved with polynomial time complexity using the standard convex optimization methods [18], [19].

5. Experimental Results

In this section, we present the experimental results on the effectiveness of the proposed accurate component model-based near-optimal residential storage control algorithm accounting for prediction errors. The PV power profiles used in our experiments are measured at Duffield, VA, in the year 2007, whereas the electric load data comes from the Baltimore Gas and Electric Company, also measured in the year 2007 [21]. We add some random peaks to the electric load profiles.

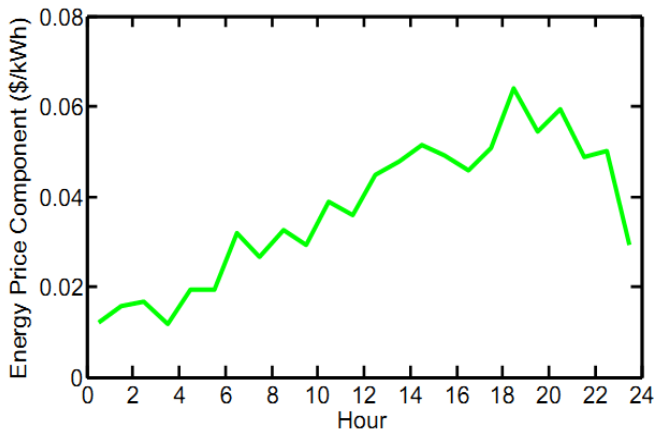

Fig. 3. The daily energy price component in the second type of electricity price function.

We use two types of electricity price functions. The first type of electricity price function is a real price function similar to [10], [11], which is given as follows. The energy price component is given by: 0.01879 $/kWh during 00:00 to 09:59 and 20:00 to 23:59, 0.03952 $/kWh during 10:00 to 12:59 and 17:00 to 19:59, 0.04679 $/kWh during 13:00 to 16:59. For the monthly demand price component, there are three price periods in a day: (i) the "high peak" period from 13:00 to 16:59, with demand price of 9.00 $/kW, (ii) the "low peak" period from 10:00 to 12:59 and from 17:00 to 19:59, with demand price of 3.25 $/kW, (iii) the "overall" period from 00:00 to 23:59 (the whole day), with demand price of 5.00/kW. The second type is a synthesized electricity price function. The energy price component over a day is demonstrated in Fig. 3. For the monthly demand price component, we consider only one "high peak" period from 18:00 to 21:59 with demand price of 9.00 $/kW, whereas the rest is "low peak" period.

We define the *cost saving capability* of a storage control algorithm (the proposed algorithm or the baseline algorithm) to be the average daily cost saving over a billing period due to the additional storage system, compared with the same residential Smart Grid user equipped only with the PV system. We compare the cost saving capabilities of the proposed near-optimal storage control algorithm with the baseline algorithm. The baseline algorithm charges the storage system from the Grid during the "off peak" period (00:00 to 09:59 and 20:00 to 23:59 in the first type of electricity price function or 00:00 to 17:59 and 22:00 to 23:59 in the second type of electricity price function) with constant charging power, and distributes energy stored in the storage system evenly in the "high peak" period.

First we show experimental results based on the first type of electricity price function. In the experiments, we set the amount of residual energy at the end of each day to be no less than 20% of the full energy capacity of the storage system. We set the inaccuracy parameter δ to be 0.8. Table I illustrates the comparison results on the cost saving capabilities between the proposed near-optimal storage control algorithm accounting for prediction inaccuracy and the baseline algorithm on every month throughout a year, when the capacity of the storage is 45 Ah. The improvement in cost saving capabilities using the proposed algorithm is provided in the table. Table II shows the comparison results on the same testing data when the capacity of the storage system is 60 Ah. We can see from these two tables that the proposed near-optimal residential storage control algorithm consistently

outperforms the baseline algorithm, with the maximum improvement of 162% (i.e., 2.62X) on the cost saving capability (on December, 45 Ah storage capacity). Furthermore, it can be observed that the proposed storage control algorithm demonstrates more significant improvement on the cost saving capability over the baseline system when the storage system has a capacity of 60 Ah. It also achieves higher cost saving capability during the winter than during the summer. The reason is that the peak load power consumption generally occurs in the "high peak" price period in the summer, and therefore, the baseline algorithm achieves relatively higher performance by distributing the storage energy only in the "high peak" periods.

TABLE I. IMPROVEMENT IN COST SAVING CAPABILITY OF THE PROPOSED ALGORITHM COMPARED WITH THE BASELINE ALGORITHM, WHEN THE STORAGE CAPACITY IS 45AH AND PARAMETER δ SET TO BE 0.8

Month	Jan.	Feb.	Mar.	Apr.
Improvement	99%	112%	69%	52%
Month	May	Jun.	Jul.	Aug.
Improvement	54%	66%	53%	59%
Month	Sep.	Oct.	Nov.	Dec.
Improvement	54%	65%	100%	162%

TABLE II. IMPROVEMENT IN COST SAVING CAPABILITY OF THE PROPOSED ALGORITHM WITH THE BASELINE ALGORITHM, WHEN THE STORAGE CAPACITY IS 60AH AND PARAMETER δ SET TO BE 0.8

Month	Jan.	Feb.	Mar.	Apr.
Improvement	159%	142%	51%	102%
Month	May	Jun.	Jul.	Aug.
Improvement	46%	61%	101%	64%
Month	Sep.	Oct.	Nov.	Dec.
Improvement	64%	127%	161%	103%

We set the parameter δ to be 1.5 and conduct the same experiments as discussed before. Table III and Table IV illustrate the comparison results when the capacity of the storage is 45 Ah and 60 Ah, respectively. We can see from these two tables that the proposed near-optimal residential storage control algorithm accounting for prediction inaccuracy consistently outperforms the baseline algorithm, with the maximum improvement of 160% (i.e., 2.60X) on the cost saving capability (on December, 45 Ah storage capacity). Moreover, when comparing with Table I and Table II, we can observe that the improvement in cost saving capability of the proposed

algorithm is slighted degraded in Table III and Table IV (i.e., when parameter δ is 1.5). This is because the prediction accuracy is lower, thereby degrading the effectiveness of the proposed near-optimal algorithm.

TABLE III. IMPROVEMENT IN COST SAVING CAPABILITY OF THE PROPOSED ALGORITHM COMPARED WITH THE BASELINE ALGORITHM, WHEN THE STORAGE CAPACITY IS 45AH AND PARAMETER δ SET TO BE 1.5

Month	Jan.	Feb.	Mar.	Apr.
Improvement	98%	82%	64%	75%
Month	May	Jun.	Jul.	Aug.
Improvement	52%	50%	44%	88%
Month	Sep.	Oct.	Nov.	Dec.
Improvement	56%	85%	53%	160%

TABLE IV. IMPROVEMENT IN COST SAVING CAPABILITY OF THE PROPOSED ALGORITHM WITH THE BASELINE ALGORITHM, WHEN THE STORAGE CAPACITY IS 60AH AND PARAMETER δ SET TO BE 1.5

Month	Jan.	Feb.	Mar.	Apr.
Improvement	112%	142%	95%	88%
Month	May	Jun.	Jul.	Aug.
Improvement	54%	48%	63%	67%
Month	Sep.	Oct.	Nov.	Dec.
Improvement	69%	48%	113%	80%

Next we show experimental results based on the second type of electricity price function. We only show experimental results on the 60 Ah storage system due to space limitation. Table V illustrates the comparison results on the cost saving capabilities between the proposed near-optimal storage control algorithm accounting for prediction inaccuracy and the baseline algorithm on every month throughout a year, when the prediction inaccuracy parameter δ is set to 0.8. Table VI illustrates the comparison results when the prediction inaccuracy parameter δ is set to 1.5. Once again, the proposed near-optimal residential storage control algorithm accounting for prediction inaccuracy consistently outperforms the baseline algorithm, with a maximum improvement of 106% on the cost saving capability. However, one can notice that the improvement is less significant than the results on the first type of electricity price function. This is because the energy cost due to the demand price component is less significant compared with that due to the energy price component in this case, which will degrade the improvement achieved by the proposed near-optimal solution (because the proposed solution is the most effective in reducing cost due to the demand price component.)

TABLE V. IMPROVEMENT IN COST SAVING CAPABILITY OF THE PROPOSED ALGORITHM COMPARED WITH THE BASELINE ALGORITHM, UNDER THE SECOND TYPE OF PRICE FUNCTION AND PARAMETER δ SET TO BE 0.8

Month	Jan.	Feb.	Mar.	Apr.
Improvement	106%	98%	65%	67%
Month	May	Jun.	Jul.	Aug.
Improvement	39%	38%	53%	49%
Month	Sep.	Oct.	Nov.	Dec.
Improvement	62%	77%	76%	91%

TABLE VI. IMPROVEMENT IN COST SAVING CAPABILITY OF THE PROPOSED ALGORITHM COMPARED WITH THE BASELINE ALGORITHM, UNDER THE SECOND TYPE OF PRICE FUNCTION AND PARAMETER δ SET TO BE 1.5

Month	Jan.	Feb.	Mar.	Apr.
Improvement	81%	105%	45%	65%
Month	May	Jun.	Jul.	Aug.
Improvement	37%	40%	43%	77%
Month	Sep.	Oct.	Nov.	Dec.
Improvement	38%	56%	68%	66%

6. Conclusion

In this paper, we address the problem of integrating residential PV power generation and storage systems into the Smart Grid for simultaneous peak power shaving and total electricity cost minimization over a billing period, making use of the dynamic energy pricing models. The residential storage control should effectively mitigate the inevitable prediction errors and properly account for the energy loss in storage charging/discharging and in power conversion circuitries. Based on the PV power generation and load power consumption prediction methods in our previous papers, we propose an accurate component model-based near-optimal storage control algorithm taking into account these aspects. We effectively implement the near-optimal storage control algorithm by solving a convex optimization problem at the beginning of each day with polynomial time complexity. Experimental results demonstrate the effectiveness of the proposed near-optimal residential storage control algorithm in electricity cost reduction compared with the baseline control algorithm.

Acknowledgements

This work is supported in part by the Software and Hardware Foundations program of the NSF's Directorate for Computer & Information Science & Engineering.

References

[1] Y. Wang, X. Lin, and M. Pedram, "Accurate component model based optimal control for energy storage systems in households with photovoltaic modules," in *Proc. of IEEE Green Technologies Conference* (GTC), 2013.

[2] L. D. Kannberg, D. P. Chassin, J. G. DeSteese, S. G. Hauser, M. C. Kinter-Meyer, R. G. Pratt, L. A. Schienbein, and W. M. Warwick, "GridWise^{TM}: The benefits of a transformed energy system," PNNL-14396, Pacific Northwest National Laboratory, Richland, Sept. 2003.

[3] S. M. Amin and B. F. Wollenberg, "Toward a smart grid: power delivery for the 21st century, " *IEEE Power and Energy Magazine*, vol. 3, no. 5, pp. 34 - 41, 2005.

[4] S. Kishore and L. V. Snyder, "Control mechanisms for residential electricity demand in SmartGrids," *Proc. of IEEE SmartGridComm*, 2010.

[5] S. Caron and G. Kesidis, "Incentive-based energy consumption scheduling algorithms for the smart grid," *Proc. of IEEE SmartGridComm*, 2010.

[6] Y. Wang, S. Yue, L. Kerofsky, S. Deshpande, and M. Pedram, "A hierarchical control algorithm for managing electrical energy storage systems in homes equipped with PV power generation," *Proc. of IEEE Green Technologies Conference* (GTC), 2012.

[7] T. Cui, Y. Wang, H. Goudarzi, S. Nazarian, and M. Pedram, "Profit maximization for utility companies in an oligopolistic energy market with dynamic prices," *Proc. of Online Green Communications Conference*, 2012.

[8] T. Esram, J. Kimball, P. Krein, P. Chapman, and P. Midya, "Dynamic maximum power point tracking of photovoltaic arrays using ripple correlation control, " *IEEE Transactions on Power Electronics*, vol. 21, no. 5, pp. 1282 - 1291, 2006.

[9] Y. Kim, N. Chang, Y. Wang, and M. Pedram, "Maximum power transfer tracking for a photovoltaic-supercapacitor energy system," *Proc. of International Symposium on Low Power Electronics and Design*, 2010.

[10] Los Angeles Department of Water & Power, Electric Rates, http://www.ladwp.com/ladwp/cms/ladwp001752.jsp.

[11] Consolidated Edison Company for New York, Inc. 2012, "Service classification no. 1 - residential and religious."

[12] T. Hiyama and K. Kitabayashi, "Neural network based estimation of maximum power generation from PV module using environmental information," *IEEE Trans. on Energy Conversion*, 1997.

[13] C. Chen, B. Das, and D. J. Cook, "Energy prediction based on resident's activity," *SensorKDD'10*, 2010.

[14] L. Wei and Z.-H. Han, "Short-term power load forecasting using improved ant colony clustering," *WKDD*, 2008.

[15] D. Linden and T. B. Reddy, *Handbook of Batteries*. McGraw-Hill Professional, 2001.

[16] M. Pedram, N. Chang, Y. Kim, and Y. Wang, "Hybrid electrical energy storage systems," in *Proc. of International Symposium on Low Power Electronics and Design* (ISLPED), 2010.

[17] D. Shin, Y. Wang, Y. Kim, J. Seo, N. Chang, and M. Pedram, "Battery-supercapacitor hybrid system for high-rate pulsed load applications," in *Proc. of Design, Automation and Test in Europe* (DATE), 2011.

[18] S. Boyd and L. Vandenberghe, *Convex Optimization*, Cambridge University Press, 2004.

[19] M. Grant and S. Boyd, "CVX: Matlab software for disciplined convex programming, version 1.21." http://cvxr.com/cvx, Feb. 2011.

[20] R. S. Sutton and A. G. Barto, *Reinforcement learning: an introduction*, MIT Press, Cambridge, MA, 1998.

[21] Baltimore Gas and Electric Company, Historical Load Data, https://supplier.bge.com/LoadProfiles_EnergySettlement/historicalloaddata.htm.

[22] A. Papoulis, Probability, *Random Variables, and Stochastic Processes*, McGraw-Hill, 2002.